NOAA Technical Report OTES 02

Simulations of the Impact of Inhomogeneous Water Columns on the Temporal Stretching of Laser Bathymeter Pulses

Rockville, Md.
August 1981

U.S. DEPARTMENT OF COMMERCE
National Oceanic and Atmospheric Administration
Ocean Technology and Engineering Services

NOAA Technical Report OTES 02

Simulations of the Impact of Inhomogeneous Water Columns on the Temporal Stretching of Laser Bathymeter Pulses

Gary C. Guenther
Engineering Development Office

Robert W. L. Thomas
EG&G/Washington Analytical Services Center, Inc.

Rockville, Md.
August 1981

U.S. DEPARTMENT OF COMMERCE
Malcolm Baldrige, Secretary

National Oceanic and Atmospheric Administration
John V. Byrne, Administrator

Ocean Technology and Engineering Services
M.E. Ringenbach, Director

Mention of a commercial company or product does not constitute an endorsement by NOAA/OTES. Use for publicity or advertising purposes of information from this publication concerning proprietary products or the tests of such products is not authorized.

CONTENTS

LIST OF FIGURES

ABSTRACT

This report documents the results of a sensitivity study to determine the potential impact of optical inhomogeneities in the water column in inducing errors in bias correctors for pulse stretching effects for a bathymetric lidar when the correctors are derived on the assumption of a homogeneous column. The existing Monte Carlo radiative transfer simulation program was modified to allow convenient simultaneous estimation of the impulse response functions for a number of different vertical distributions of scatterers and absorbers. Outputs were obtained for vertical optical depths up to 16, six different values of single-scatter albedo, and two nadir angles in air -- namely, 0 and 25 degrees. A digital convolution was performed over an anticipated source pulse profile to obtain the "environmental response functions" (ERF's), and biases were estimated by applying the same linear fractional threshold to both the source pulse and the ERF and comparing the results to the actual simulated depths. The results for the inhomogeneities we considered indicate that the use of correctors derived for the homogeneous case is likely to result in errors of less than 10 cm.

1.0 INTRODUCTION

Analytical studies of the propagation-induced pulse stretching effects by Thomas and Guenther (1979) pointed to the need for quantitative estimates of the depth measurement biases for a bathymetric laser sounder. These biases are larger than allowed in international hydrographic standards. Monte Carlo simulations were created (Guenther and Thomas 1981a,b) to compute more accurate estimates of the biases for use as depth correctors.

The simulations that were performed were for homogeneous scattering media only. In other words, it was assumed that the density and nature of the scattering particles in water are independent of depth. There is some evidence (Swift 1977) to indicate that significant departures from a homogeneous description may occur frequently in coastal waters. It is important, therefore, to assess the potential for error in using homogeneous case corrections when departures from homogeneity occur.

The work described here involved a modification of the existing Monte Carlo simulation code to compute the impulse response functions (IRF's) for both homogeneous and inhomogeneous water columns simultaneously. The resulting IRF's were convolved with a typical source pulse to produce the "environmental response functions" (ERF's). Linear fractional threshold pulse locators were applied to the ERF's to determine the bias errors and the differences in bias errors between the homogeneous case and the various inhomogeneous models.

Section 2 of this report discusses the analytical formulations and programming developments undertaken as part of this task; Section 3 discusses the specific parameters employed in the study and details results. Conclusions are given in Section 4.

2.0 SIMULATION OF THE TRANSPORT OF LIGHT THROUGH INHOMOGENEOUS WATER COLUMNS

2.1 The Relevant Physical Processes

The fundamental mechanism of transport through an inhomogeneous column is the same as that for the homogeneous case. The incident ray is refracted at the surface, and photons entering the water are subject to both scattering and absorption. Those photons that survive scattering events travel to the bottom where they are reflected, and a small fraction of the reflected photons are scattered back to the surface in a direction such that they are refracted in the direction of the receiver.

While there exists data on the vertical turbidity profile for some waters (Swift 1977), there is little data on the variability of the character of the scatterers. The simplest initial assumption is that the scattering and absorbing species remain invariant both in character and relative density and are merely redistributed through the water column in different ways. This assumption aids the conceptual interpretation of the results since only one aspect of the medium is affected. Further, there exists a straightforward conversion of the previous simulation code to allow the treatment of inhomogeneities of this type, and there are computational advantages in that different inhomogeneities can be examined simultaneously.

Figure 1 illustrates schematically the spatial dispersion for three cases:

1. a homogeneous water column;

2. a water column with a higher concentration of scatterers and absorbers near the surface; and

3. a water column with scatterers and absorbers concentrated near the bottom.

In the homogeneous case the dispersion of the beam increases at a uniform rate with increasing depth, while, for case 2, the majority of the dispersion occurs in the surface layer. The beam divergence is therefore large for most of the depth in the latter case which leads to increased pulse stretching compared to the homogeneous case. In case 3 very little dispersion occurs over most of the depth since the scatterers are concentrated near the bottom, and, in this case, the pulse stretching will be reduced compared to the homogeneous case.

A review of Figure 1 indicates that the most serious departures from the homogeneous case are likely to occur when there are high densities of scatterers and absorbers near the surface or near the bottom. We therefore elected to perform simulations for two-layer systems with these characteristics.

2.2 The Simulation Method

The Monte Carlo method is used to simulate the transport of representative photons through the water column to the bottom. We consider photons incident on the surface at time, t=0, in a direction making an angle, ψ, with the nadir. The surface at the point of incidence is considered to be horizontal so that the nadir angle of transport immediately beneath the surface is given by Snell's Law:

$$\sin \phi = \frac{\sin \psi}{\mu} , \tag{1}$$

where μ is the refractive index of water for green light (1.33).

The mean free path through water is traditionally described by the "narrow beam attenuation coefficient" (α), where $\alpha\, dz$ is the probability that a photon will be absorbed or scattered in travelling through a distance dz. If "a" and "s" are the absorption and scattering coefficients, then, by definition,

$$\alpha = a + s . \tag{2}$$

In an inhomogeneous medium, α, a, and s all vary with location. Nevertheless, we assume that they vary in proportional fashion since the character and relative densities of the species are assumed to be invariant. Thus, the "albedo for single scattering," ω_0, defined by

$$\omega_0 = \frac{\alpha - a}{\alpha} = \frac{s}{\alpha} \tag{3}$$

is assumed to be invariant with depth. ω_0 is the fractional number of photons entering encounters which are not absorbed; it is used as a scalar multiplier of the photon weight at each encounter.

To determine the path length between scatterings we define the optical path length, τ, as

$$\tau = \int_0^x \alpha(\ell)\, d\ell\,, \tag{4}$$

where x is the distance travelled since the last encounter. The optical path length τ is obtained at random from the probability distribution

$$p(\tau)\, d\tau = e^{-\tau}\, d\tau \tag{5}$$

by setting the value of τ to

$$\tau = -\ell n\, \rho\,, \tag{6}$$

where ρ is a rectangularly distributed random number between 0 and 1. Equation (4) is then solved to compute the path length, x.

Since the character of the scatterers is invariant, we can regard the directions of travel of photons between scatterings as being independent of the density distribution of scatterers. Thus, for all the models treated, we can think of the photon paths between the nth and (n+1)th scatterings as having the same direction cosines. This is a very important concept since it allows us to evaluate the impact of different inhomogeneities with a minimal increase in computer time.

Figure 2 illustrates the procedure for estimating the depth of a scattering event for a single two-layer model. The first step is to estimate the optical depth of the scattering, τ_S, from the surface. This is simply the sums of the optical paths, τ, weighted by the cosines of the associated nadir angles. We then refer to the plot of the optical depth to the surface for the given inhomogeneity model and compute the true depth of the event. The depth difference between successive scattering events divided by the absolute value of the cosine of the nadir angle then gives the path length.

It is apparent that, for a given vertical optical depth, we can readily estimate the temporal distributions of photons arriving at the bottom for several different vertical inhomogeneties simultaneously by using the same scattering computations and merely scaling appropriately to compute

the true time delays relevant to the various inhomogeneities for each sampled photon. Therefore, we organized our computations to obtain results for fixed <u>total</u> optical depths with several distributions of scatterers and absorbers for each. The total optical depth of the water column is given by $\int_0^D \alpha(z)\, dz$, where dz is an incremental vertical element at depth, z, but, for the sake of compactness we have retained the use of "αD" as a notation for the total integrated optical depth.

Photons are considered to change direction at all scattering events. The scattering angle θ from the incident direction is generated according to the "phase function," $P(\theta)$, which defines the probability that the photon will scatter into a unit solid angle between θ and $\theta+d\theta$. Since the solid angle between θ and $\theta+d\theta$ is $2\pi \sin\theta\, d\theta$, the probability of occurence of θ in θ to $\theta+d\theta$ is

$$p'(\theta)\, d\theta = 2\pi \sin\theta\, P(\theta)\, d\theta. \qquad (7)$$

The value of each scattering angle, θ_k, is generated by solving the equation

$$\int_0^{\theta_k} p'(\theta)\, d\theta = 4\pi\, \rho\ , \qquad (8)$$

where ρ is a rectangularly distributed random number between 0 and 1. This equation is solved by linear interpolation within a look-up table of the value of the integral as a function of θ_k.

The lengths of the photon paths for the photons reaching the bottom are summed to allow an evaluation of the associated time delay. The minimum time of transit to the bottom is

$$t_W = \frac{D}{c_W} \quad , \tag{9}$$

where c_W is the velocity of light in water. The "time delay" for paths of length L_i is then computed as

$$t_D = \frac{1}{c_W} \left(\sum_{i=1}^{n} L_i - D \right). \tag{10}$$

By repeating this computation for a large number of downwelling photons we can compute the downwelling impulse response function $d(t_D)$ as a histogram representing the probability distribution of arrival times of incident photons at the bottom.

For given values of αD and ω_0, all temporal results scale linearly with the depth, D. If we consider representative photon paths for two cases with the same αD but with different values of D, the photon paths are geometrically "similar" so that the fractional time delays t_D/t_W, are identical. Therefore the absolute time delays scale linearly with D, and one set of simulated results can be used to determine absolute results for all depths.

In order to increase the efficiency of the simulations further, we sample the times of first crossings of a number of intermediate levels on the way to the bottom. The intermediate levels are characterized by the appropriate values of total optical depth. Because of the above scaling law we are able to arbitrarily set to unity the depth D_{max} corresponding to the largest value of αD, namely, αD_{max}.

The impulse response at a distant receiver is estimated using the "reciprocity" principle (Chandrasekhar 1960) which implies that the statistical description of the simulated downwelling photon tracks can be regarded as representative for both downwelling and upwelling photons. Thus the computed impulse response $d(t_D)$ for downwelling transport forms the basis for the determination of the two-way impulse response.

If the bottom reflection were regarded as isotropic, then reflection into a given solid angle in every direction would be equally likely. In this case we could estimate the receiver response function by regarding $d(t_D)$ to be the distribution function describing both downwelling and upwelling radiation. Very little data exists on the actual directional reflectivity of the ocean bottom, so in earlier simulations (Guenther and Thomas 1981a) we chose the traditional approach of assuming that the bottom is a Lambertian reflector; i.e., that the probability of reflection at a zenith angle Z is proportional to cos Z. This type of reflection results in a uniformly bright appearance of the illuminated surface independent of the viewing angle in the absence of the turbid medium. In the present simulations, however, we saved computer storage space by assuming isotropic bottom

reflection so that the impulse response function for upwelling photons, $u(t_D)$, was taken to be identical to $d(t_D)$. The result of this assumption is not very different from that of the Lambertian assumption. The sampled function $u(t_D)$, is considered to characterize the airborne receiver response for photons released from the bottom (all at time t=0). Just as for $d(t_D)$, the minimum time for any sample $u(t_D)$ is t_w given by Eq. (9).

We compute the receiver response function r(T) at a time T following the earliest possible round-trip return. We note that if this return arises from downwelling photons with a time delay t_1, then the value of t_2, the time delay required for the upwelling path, is $T-t_1$. Thus the value of r(T) can be expressed by the integration of the product of $d(t_1)$ and $u(t_2)$ over all such cases:

$$r(T) = \int_0^T d(t_1)\, u(T-t_1)\, dt_1. \tag{11}$$

This is, of course, the convolution of u over d. The functions u and d are actually constructed by discrete samples during an interval $\Delta \cdot t_w$ where Δ is a small fraction (typically 0.005), and t_w, as before, is the vertical transit time for unscattered photons. The function r(t) is then constructed for discrete values of $T=nt_w\Delta$ (where n is an integer) by the following digital convolution of d and u:

$$r(n) = \sum_{m=1}^{n} d(m)\, u(n-m+1), \tag{12}$$

where d(m) is the sample of d collected such that

$$(m-1)t_w\Delta \leq t_D < m\ t_w\Delta, \qquad (13)$$

and similarly for u(m). The value of r computed in this way has an associated time unit of $t_w\Delta$.

The act of convolving the functions d and u is an integration, and, as such, it has the effect of reducing the magnitude of statistical noise in the resulting function. It has been found that the function r(T) is acceptably reproducible for simulations of as low as 10,000 photons when the program is rerun with different starting random numbers; this adds confidence to the results.

When the time increment Δ is set to 0.005, the maximum time delay sampled is 0.25 t_w (=50 $t_w\Delta$). This means that only that part of the return occurring with a time delay (over the vertical two-way transit time) less than one quarter of the depth transit time is generated. This is normally the region within which the peak of the return power occurs. The restriction of considering only the delay times up to 0.25 t_w is important in limiting the simulation time requirements since any photons that were delayed by more than these amounts (compared to radiation travelling vertically downwards) can be eliminated from the simulations.

The "reference time", T_R, for the computation of depth measurement bias errors is the time delay for radiation travelling unscattered (at the refraction angle ϕ) to the bottom and then being

reflected back along the same path. This time delay is

$$T_R = 2t_w \, (\sec \phi - 1). \tag{14}$$

For the nadir case, of course, ϕ is zero, so that T_R is zero. Thus only positive (deep) errors in depth estimates can be contributed by propagation effects in this case. For the off-nadir cases, however, both positive and negative errors can occur. Negative (shallow) errors arise from a favoring of paths closer to vertical, since these are the ones for which absorption is less likely to occur. This is the so-called "undercutting" effect where bottom reflection occurs predominantly "beneath" the unscattered ray, and a significant amount of energy is returned before the reference delay time, T_R, as illustrated in Fig. 1.

Although a specific receiver field of view is not directly applied in the simulation, an effective field-of-view restriction is caused by the truncation of paths which have been judged to be excessively long (by the previously mentioned time increment criterion). This restriction applies only to photons which would have arrived in the trailing edge of the impulse response and in no way affects the leading edge or the peak power. Thus, the effective field of view is large but considerably less than unlimited, and probably represents a fairly realistic situation.

2.3 Interpretation of the Results

2.3.1 Environmental Response Functions

The simulations generate impulse response functions for the receiver as a function of the albedo for single scattering, ω_0, and the vertical optical depth, αD, for each inhomogeneity model considered. All results are normalized such that

1. the input energy is unity,

2. the depth transit time is unity, and

3. the sampling interval is Δ.

The peak power of the impulse response function, P_r, is the sampled energy for a time interval that in the real world is $t_w\Delta$. Thus, if r_{max} is the peak power in units of energy/second, we have

$$r_{max} = \frac{P_r}{t_w\Delta} \quad . \tag{15}$$

In practice, of course, the input laser pulse is not an impulse but is distributed over time. Let s(t) represent the laser output power as a function of time (in watts), and let S(joules) be the total output energy of the pulse. Then

$$S = \int_0^\infty s(t)\, dt \,. \tag{16}$$

The true response of the receiver, v(T), at time T following the earliest possible round trip return is given by the convolution of s(t) over r(t), the impulse response function; i.e.,

$$v(T) = \int_0^T s(t)\, r(T-t)\, dt \,. \tag{17}$$

In constructing v(T), care must be taken to insure that r(T-t) is scaled to be appropriate to the depth of interest. For given values of αD and ω_0 and a given inhomogeneity, the time scale for r(T-t) scales linearly with the depth. The function v(T) is the "environmental response function" (ERF).

The total return energy is given by

$$V = \int_0^\infty v(T)\, dT \,. \tag{18}$$

Remembering that r(t) = s(t) = 0 for all t less than zero, it is easy to show by Eqs. (17) and (18) that

$$V = SR, \tag{19}$$

where R is the integrated impulse response function, which simply states that the total return energy is the total input pulse energy multiplied by the return energy per unit input.

2.3.2 Bias Estimation

In computing the results for the bias, we first estimate T_f, the difference between the time, T_{vf}, that the environmental response function v(T) rises through a fraction, f, of its peak value and the time, T_{sf}, when the source pulse, s(t), (representing the surface return) rises through the same fraction of its peak. Since s(t) was assumed to be triangular in shape with a rise time of $\frac{B}{2}$, where B is the base width of the triangle (Miller 1981), we have

$$T_{sf} = \frac{1}{2} fB. \tag{20}$$

Then, remembering that the unscattered ray has an associated delay time of T_R, given by Eq. (14), we obtain the bias as

$$T_E = T_{vf} - \frac{1}{2} fB - T_R. \tag{21}$$

The related depth error is

$$E = \frac{T_E c_w}{2 \sec \phi}, \tag{22}$$

where c_w is the velocity of light in water (=22.5 cm/ns), and ϕ is the nadir angle of the unscattered ray in the water.

2.4 Program Validation

In organizing the storage and processing of sampled photons, two data structures evolved. The first was identical to that employed in the estimation of biases for homogeneous water columns (Guenther and Thomas 1981a), while the second was specially created to handle the inhomogeneous cases. The coding for the homogeneous case estimation was left unchanged, while new coding was developed to handle the inhomogeneous cases.

In an early test of the code we set the parameters of one of the inhomogeneous models to be such that the scatterer and absorber densities were equal in the two layers. Thus, one of the "inhomogeneous" cases actually described the same density distribution as the homogeneous case. Since the same simulated photons were used to generate the results for the two models, the outputs for the two cases should have been identical. Inspection of the output files validated that this was indeed the case. Moreover, these results agreed very closely with those generated in the earlier study for the homogeneous case assuming Lambertian reflection at the bottom (Guenther and Thomas 1981a). Those, in turn, had been validated through internal consistency checks and agreement of computed apparent water properties with the work of previous authors (Timofeyeva 1972; Gordon, Brown, and Jacobs 1975).

3.0 DISCUSSION OF RESULTS

The impulse response functions (IRFs) for the receiver with a wide field of view were estimated by the Monte Carlo program and archived on disk storage. In a later post-processing step, the IRFs were scaled to the depth of interest and convolved with the source pulse, s(t), to produce the environmental response functions (ERFs). The ERFs were then processed to compute the required biases, and a subset of both the ERFs and the computed biases were archived on disk for later use.

The emphasis in this report is the sensitivity of the bias results to inhomogeneities in the water column. The most important results, therefore, are the differences between the depth biases computed for the inhomogeneous case and those for the homogeneous case. However, since the biases relating to the ERFs have not been reported before, we also report the depth-specific biases for the homogeneous case. The depth chosen for the presentation of output was 20m since this is the greatest depth at which the international standards require an accuracy of ± 1 foot (30 cm).

3.1 The Cases Treated

Since we were concerned primarily with bounding the sensitivities in this study, the set of parameters employed was more limited than that for the homogeneous case. The input parameters to the simulation are listed in Table 1.

TABLE 1

List of parameters over which results were computed:

1. Scattering phase function, $P(\theta)$:
   "NOS" or "dirty"

2. Nadir angle of entry in air, ψ(Degrees):
   0, 25

3. αD = vertical optical depth of water column (Dimensionless):
   2, 4, 6, 8, 10, 12, 14, 16

4. ω_0 = albedo of single scattering:
   0.93, 0.9, 0.8, 0.6, 0.5, 0.4

5. Distributions of scatterers and absorbers:

   a) Homogeneous
   b) Surface layer with double the ambient density
   c) Surface layer with four times the ambient density
   d) Bottom layer with double the ambient density
   e) Bottom layer with four times the ambient density

   (Layer thickness = one tenth of depth in all cases)

6. Depth = 20 m. Total width of source pulse = 14 ns.

The "NOS" phase function is appropriate to "dirty" water and the associated volume scattering function for this case was taken from the work of Petzold (1972). The selected nadir angles of 0 and 25 degrees bound the anticipated operational range, while the set of vertical optical depths is identical to that employed in the earlier study of the homogeneous case. Only six single-scattering albedo values were used (compared to eight previously), but we did include the new value, 0.93, which may be appropriate for some coastal waters. The base width B of the source pulse was taken to be 14 ns (Miller 1981).

For each value of ψ, αD, and ω_0, five vertical distributions of scatterers were considered with relative densities as shown on the left-hand side of Fig. 3. The first model was the homogeneous case; models 2 and 3 had a surface layer with 2 and 4 times the ambient density, respectively; models 4 and 5 had a bottom layer with 2 and 4 times the ambient density.

The listed output includes the following for all cases:

1. the impulse response function for downwelling radiation reaching the bottom;

2. the convolution of function (1) over itself, representing the result at the receiver; and

3. the spatial (radial and Cartesian) distributions of the downwelling radiation at the bottom.

3.2 The Biases and Bias Sensitivities

Appendix A contains the output of the post-processing program summarizing the computed biases for linear fractional thresholds of 10, 20, 50 and 80 percent applied to the ERFs computed for a depth of 20m. For the homogeneous case, we present the actual biases, E, given by equation (22), while, for the inhomogeneous models, the tables give the differences between the computed biases and the corresponding values for the homogeneous case.

The first observation to be made is that for most cases of interest, convolving the source pulse over the IRF results in a considerably reduced sensitivity of the biases to both ω_0 and αD compared to the sensitivity for limiting biases calculated from the impulse responses alone. Further, since the linear fractional threshold is applied to both the source pulse and the ERF, the bias is insensitive to the value of the fractional threshold as long as the IRF is short compared to the source pulse.

For the nadir case, deep biases over one foot (30 cm) occur only for an αD value of 16. As expected, the biases increase with increasing ω_0 and αD. The impact of the surface layer is to increase the bias but only very slightly -- never more than about 2 cm. With the bottom layer, the result is generally to reduce the bias. The maximum error in the use of the homogeneous corrector is seen to be about 7 cm. As expected, the impact of the inhomogeneity generally increases when the layer density increases.

For the case where the nadir angle is 25 degrees, an underestimate of about 60 cm is observed in all cases, with an increasing underestimate for the surface layer models and a diminishing underestimate for the bottom layer models being the general rule. The error in using the homogeneous case assumption here, however, is seen never to exceed about 5 cm.

The rise times of the ERFs are also listed. These always increase with increasing αD and ω_0 but show virtually no sensitivity to any of the inhomogeneities treated. As expected, a very slight increase occurs for the surface layer case, and a slight decrease appears when the layer is near the bottom.

The closeness of the results for the inhomogeneous cases to those for the homogeneous medium are best understood by reviewing the graphs of integrated optical thickness from the surface as a function of depth as given on the right-hand side of Fig. 3. These are the graphs actually used in determining the true depths of the scattering points from their optical depths. It can be seen that the separations of the plots for the inhomogeneous cases from the homogeneous case are not very large although the layer densities are substantially different from the ambient densities. The result is that the photon paths for the inhomogeneous cases are never displaced physically very far from those of the homogeneous case, and the IRFs must therefore be similar.

4.0 CONCLUSIONS

The Monte Carlo propagation simulation code was modified to permit the investigation of the effects of an inhomogeneous water column on the impulse response functions and on bias correctors determined by the application of linear fractional threshold pulse locators to the resulting environmental response functions. A number of inhomogeneous models were simulated with layers of "dirty" water near the surface or near the bottom. For a bounding set of system parameters and optical properties, the changes in the bias correctors (compared to the homogeneous case) were never larger than 8 cm at a 20-m depth. It is our judgment, therefore, that reasonable water column inhomogeneities in nature will not cause a significant change in the bias correctors required to remove the effects of underwater propagation from airborne lidar bathymetric measurements.

REFERENCES

Chandrasekhar, S., 1960: Radiative Transfer. Dover Publications, New York, N.Y., 385pp.

Gordon, H.R., Brown, O.B., Jacobs, M.M., 1975: Computed relationships between the inherent and apparent optical properties of a flat homogeneous ocean, Appl. Opt., 14, 417-427.

Guenther, G.C., and Thomas, R.W.L., 1981a: Monte Carlo simulations of the effects of underwater propagation on the penetration and depth measurement bias of an airborne laser bathymeter. NOAA Technical Memorandum OTES 01, National Oceanic and Atmospheric Administration, U.S. Department of Commerce, Washington, D.C., 144pp.

Guenther, G.C. and Thomas, R.W.L., 1981b: Error analysis of pulse location estimates for simulated bathymetric lidar returns. NOAA Technical Report OTES 01, National Oceanic and Atmospheric Administration, U.S. Department of Commerce, Washington, D.C., 51pp.

Miller, M., 1981: Private communcation.

Petzold, T.J., 1972: Volume scattering functions for selected ocean waters. SIO Ref. 72-78, Scripps Institution of Oceanography, San Diego, Ca., 79pp.

Swift, R.N., 1977: Preliminary report on pre-flight sea-truthing for the Airborne Oceanographic Lidar Project. Marine Science Consortium, Wallops Island Marine Science Center, Wallops Island, Virginia, 102pp.

Thomas, R.W.L., and Guenther, G.C., 1979: Theoretical calculations of bottom returns for bathymetric lidar. Proceedings of the International Conference on Lasers '78, Orlando, Fla., 48-59.

Timofeyeva, V.A., 1972: Relations between certain optical properties in turbid media with different scattering patterns. Isv., Atmospheric and Oceanic Physics (Acad. of Sci., USSR), 8, 895-896.

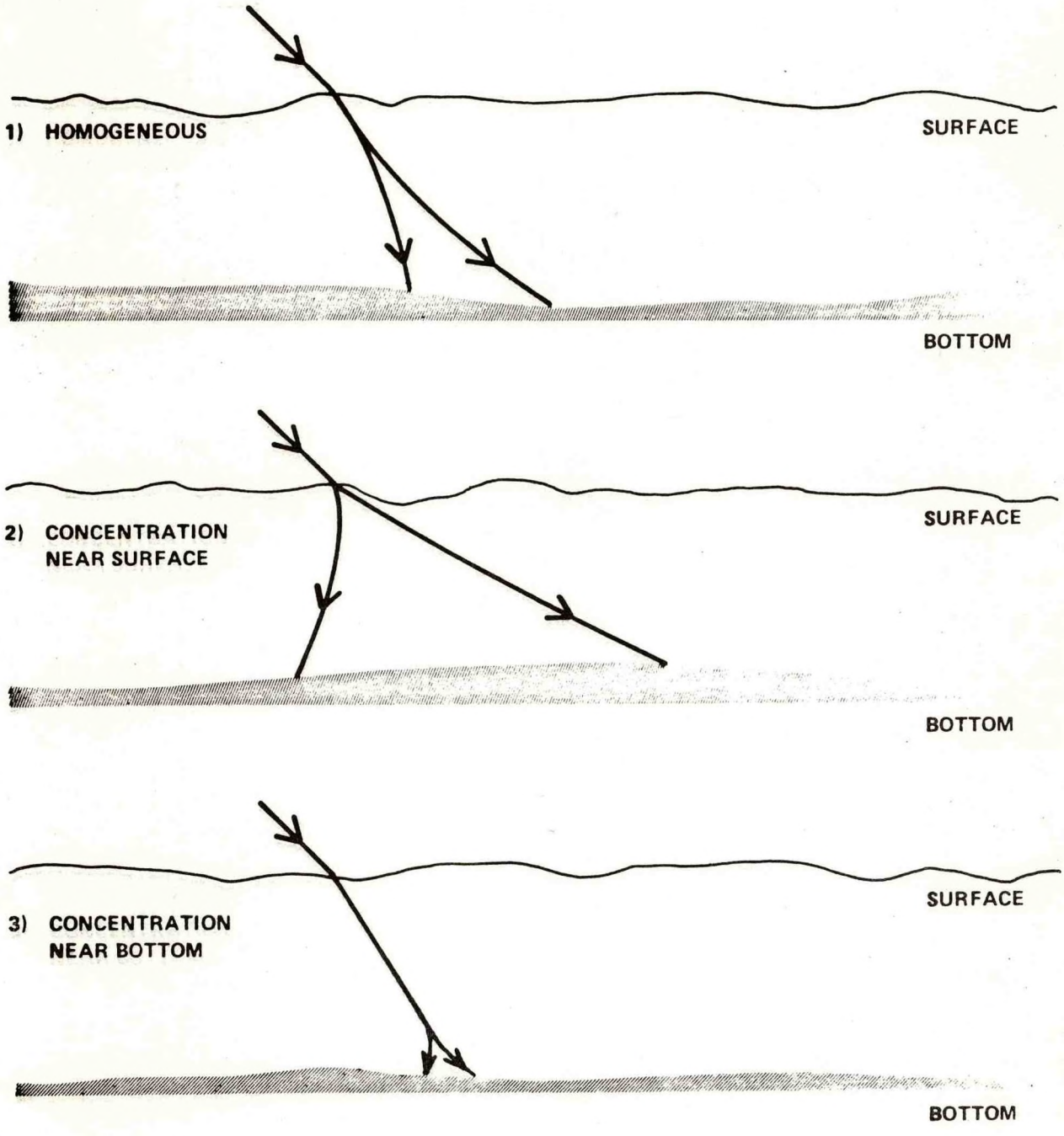

FIGURE 1. GENERAL EFFECTS OF INHOMOGENEITIES ON BEAM DISPERSION

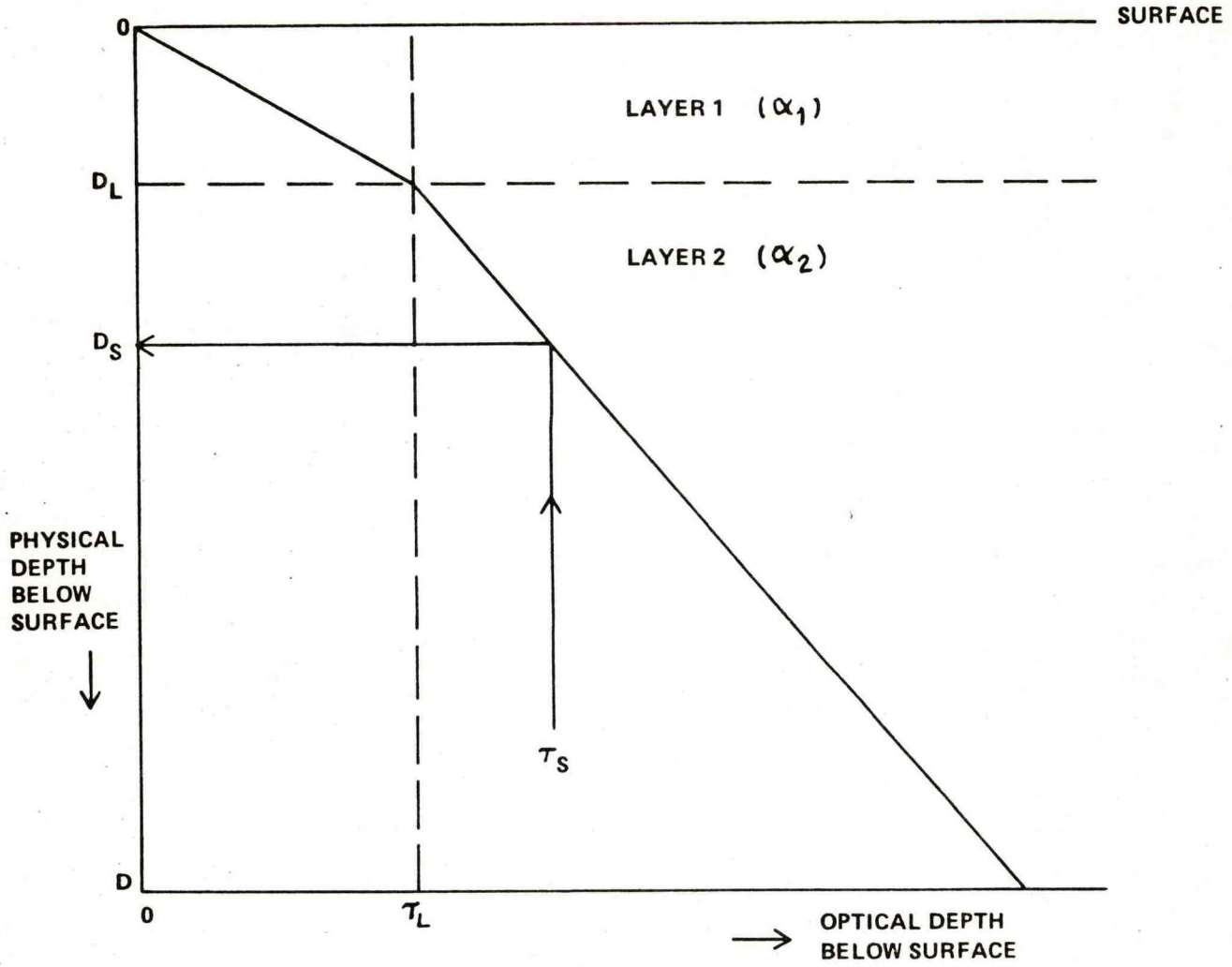

τ_S = OPTICAL DEPTH OF SCATTERING POINT BELOW SURFACE

D_S = ACTUAL DEPTH OF SCATTERING POINT BELOW SURFACE

FIGURE 2. METHOD OF COMPUTING LOCATION OF SCATTERING POSITION

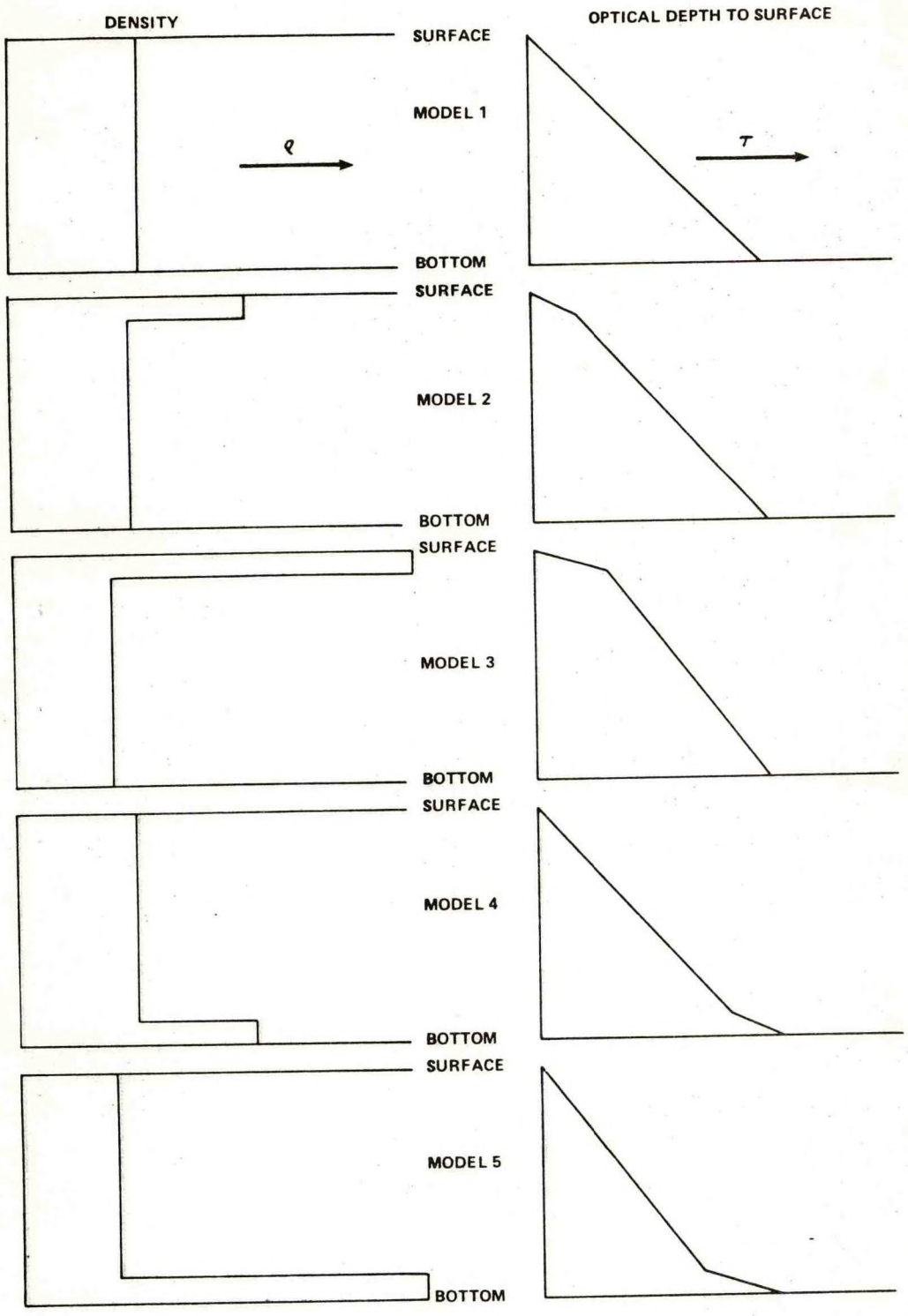

FIGURE 3. SCATTERING PARTICLE DENSITY AND OPTICAL DEPTH TO THE SURFACE

APPENDIX A
TABULAR RESULTS FOR BIASES, PULSE RISE TIMES, AND THE CHANGES INDUCED BY INHOMOGENEITIES

convolution summary for NOS water

zenith angle of entry= 0.00 degrees DEPTH= 20.00 METERS

INHOMOGENEITY MODEL NO. 1 RESULTS ARE FOR ABSOLUTE BIASES AND RISE TIMES

bias in 10 percent point (CENTIMETERS)

alpha*d=	2.000	4.000	6.000	8.000	10.000	12.000	14.000	16.000
albedo								
0.93	1.858	4.358	7.180	10.304	14.437	18.236	21.508	25.148
0.90	1.782	4.179	6.844	9.834	13.740	17.441	20.557	23.776
0.80	1.538	3.595	5.803	8.220	11.635	15.203	17.501	19.512
0.60	1.105	2.489	4.003	5.599	8.136	11.601	12.700	12.550
0.50	0.893	1.962	3.168	4.436	6.781	10.357	11.043	10.513
0.40	0.683	1.468	2.359	3.257	5.769	9.311	9.809	9.310

bias in 20 percent point (CENTIMETERS)

alpha*d=	2.000	4.000	6.000	8.000	10.000	12.000	14.000	16.000
albedo								
0.93	2.628	5.977	9.834	13.538	18.291	22.620	26.454	30.737
0.90	2.520	5.751	9.395	12.923	17.504	21.704	25.283	29.198
0.80	2.173	5.004	8.017	10.934	14.929	18.870	21.812	24.315
0.60	1.558	3.527	5.619	7.498	10.565	14.546	15.815	15.915
0.50	1.248	2.793	4.512	5.923	8.799	12.950	13.668	13.216
0.40	0.941	2.092	3.401	4.426	7.413	11.616	12.010	11.562

bias in 50 percent point (CENTIMETERS)

alpha*d=	2.000	4.000	6.000	8.000	10.000	12.000	14.000	16.000
albedo								
0.93	2.525	6.235	10.484	14.867	20.295	24.982	29.042	34.041
0.90	2.391	6.002	9.978	14.126	19.338	23.828	27.684	32.250
0.80	1.972	5.213	8.391	11.723	16.259	20.420	23.546	26.551
0.60	1.313	3.571	5.763	7.759	11.066	15.222	16.893	16.941
0.50	0.980	2.706	4.611	5.990	9.098	13.366	14.624	13.861
0.40	0.646	1.879	3.396	4.434	7.661	11.781	12.772	11.929

bias in 80 percent point (CENTIMETERS)

alpha*d=	2.000	4.000	6.000	8.000	10.000	12.000	14.000	16.000
albedo								
0.93	0.618	3.307	7.002	11.244	17.140	22.896	28.317	34.949
0.90	0.515	3.146	6.535	10.514	15.987	21.392	26.489	32.581
0.80	0.212	2.593	5.093	8.183	12.600	17.275	21.062	24.937
0.60	-0.131	1.393	2.978	4.636	7.551	11.649	13.055	13.165
0.50	-0.305	0.741	2.148	3.191	5.792	9.820	10.769	9.995
0.40	-0.482	0.156	1.247	2.092	4.621	8.281	8.973	8.189

rise time from one percent point to peak (ns)

alpha*d=	2.000	4.000	6.000	8.000	10.000	12.000	14.000	16.000
albedo								
0.93	7.297	7.256	8.539	8.912	10.120	10.385	10.669	11.422
0.90	7.298	7.259	8.101	8.923	9.697	9.978	10.705	11.035
0.80	6.857	7.269	7.676	8.513	9.315	9.634	9.974	10.306
0.60	6.864	7.287	7.263	7.677	8.068	8.871	8.846	9.252
0.50	6.867	7.295	7.276	7.255	8.097	8.467	8.461	8.423
0.40	6.871	6.858	7.289	7.276	7.674	8.055	8.507	8.009

convolution summary for NOS water

zenith angle of entry= 0.00 degrees DEPTH= 20.00 METERS

INHOMOGENEITY MODEL NO. 2 RESULTS ARE RELATIVE TO THE HOMOGENEOUS CASE

bias in 10 percent point (CENTIMETERS)

alpha*d=	2.000	4.000	6.000	8.000	10.000	12.000	14.000	16.000
albedo								
0.93	0.023	0.025	0.042	0.084	0.410	0.333	0.615	0.228
0.90	0.022	0.023	0.034	0.078	0.418	0.334	0.625	0.222
0.80	0.016	0.017	0.031	0.081	0.344	0.350	0.644	0.114
0.60	0.010	0.009	0.024	0.062	0.265	0.436	0.588	0.198
0.50	0.007	0.007	0.016	0.049	0.236	0.416	0.438	0.296
0.40	0.005	0.003	0.004	0.029	0.200	0.499	0.157	0.327

bias in 20 percent point (CENTIMETERS)

alpha*d=	2.000	4.000	6.000	8.000	10.000	12.000	14.000	16.000
albedo								
0.93	0.030	0.048	0.083	0.107	0.481	0.274	0.604	0.483
0.90	0.030	0.044	0.067	0.090	0.469	0.305	0.647	0.423
0.80	0.020	0.032	0.055	0.070	0.473	0.413	0.592	0.276
0.60	0.015	0.014	0.042	0.037	0.391	0.576	0.830	0.274
0.50	0.011	0.008	0.032	0.014	0.368	0.576	0.895	0.322
0.40	0.007	-0.001	0.015	0.000	0.333	0.657	0.917	0.313

bias in 50 percent point (CENTIMETERS)

alpha*d=	2.000	4.000	6.000	8.000	10.000	12.000	14.000	16.000
albedo								
0.93	0.049	0.049	0.126	0.204	0.509	0.270	0.647	0.535
0.90	0.047	0.047	0.100	0.181	0.489	0.287	0.707	0.510
0.80	0.026	0.039	0.089	0.155	0.484	0.377	0.672	0.400
0.60	0.017	0.028	0.077	0.109	0.378	0.530	0.813	0.457
0.50	0.013	0.024	0.066	0.063	0.331	0.473	0.812	0.616
0.40	0.009	0.008	0.044	0.031	0.187	0.571	0.671	0.701

bias in 80 percent point (CENTIMETERS)

alpha*d=	2.000	4.000	6.000	8.000	10.000	12.000	14.000	16.000
albedo								
0.93	0.038	0.067	0.151	0.174	0.614	0.359	0.659	1.092
0.90	0.037	0.065	0.108	0.148	0.605	0.399	0.780	0.914
0.80	0.011	0.059	0.077	0.133	0.503	0.481	0.754	0.556
0.60	0.009	0.045	0.052	0.108	0.427	0.598	0.914	0.324
0.50	0.007	0.038	0.050	0.062	0.400	0.523	0.959	0.506
0.40	0.005	0.013	0.042	0.039	0.242	0.642	0.726	0.590

rise time from one percent point to peak (ns)

alpha*d=	2.000	4.000	6.000	8.000	10.000	12.000	14.000	16.000
albedo								
0.93	-0.000	-0.000	-0.002	0.441	-0.006	-0.010	0.421	-0.003
0.90	-0.000	-0.000	-0.001	-0.003	-0.005	0.435	-0.021	0.442
0.80	-0.000	-0.000	-0.001	-0.002	-0.002	-0.010	-0.026	0.440
0.60	-0.000	-0.000	-0.001	-0.001	0.446	-0.007	0.433	-0.002
0.50	-0.000	-0.000	-0.001	-0.000	0.003	-0.005	0.438	-0.000
0.40	-0.000	-0.000	-0.000	-0.000	0.004	0.440	0.444	0.001

convolution summary for NOS water

zenith angle of entry= 0.00 degrees DEPTH= 20.00 METERS

INHOMOGENEITY MODEL NO. 3 RESULTS ARE RELATIVE TO THE HOMOGENEOUS CASE

bias in 10 percent point (CENTIMETERS)

alpha*d= albedo	2.000	4.000	6.000	8.000	10.000	12.000	14.000	16.000
0.93	0.048	0.043	0.131	0.238	0.529	0.668	1.117	0.694
0.90	0.046	0.040	0.117	0.224	0.559	0.657	1.088	0.762
0.80	0.033	0.030	0.102	0.247	0.468	0.594	1.121	0.566
0.60	0.021	0.013	0.063	0.194	0.375	0.572	1.042	0.934
0.50	0.015	0.007	0.042	0.160	0.295	0.512	0.865	1.339
0.40	0.010	-0.000	0.020	0.091	0.199	0.538	0.616	1.819

bias in 20 percent point (CENTIMETERS)

alpha*d= albedo	2.000	4.000	6.000	8.000	10.000	12.000	14.000	16.000
0.93	0.067	0.062	0.159	0.298	0.613	0.716	1.227	1.166
0.90	0.065	0.059	0.133	0.271	0.605	0.740	1.308	1.108
0.80	0.047	0.048	0.099	0.270	0.597	0.782	1.185	0.875
0.60	0.036	0.030	0.041	0.190	0.472	0.780	1.527	0.978
0.50	0.029	0.022	0.030	0.136	0.399	0.757	1.692	1.285
0.40	0.022	0.010	0.011	0.091	0.291	0.829	1.845	1.622

bias in 50 percent point (CENTIMETERS)

alpha*d= albedo	2.000	4.000	6.000	8.000	10.000	12.000	14.000	16.000
0.93	0.089	0.080	0.338	0.476	0.628	0.847	1.417	1.346
0.90	0.086	0.076	0.302	0.429	0.618	0.861	1.437	1.367
0.80	0.049	0.066	0.272	0.411	0.600	0.860	1.415	1.233
0.60	0.037	0.052	0.175	0.290	0.482	0.803	1.629	1.327
0.50	0.031	0.047	0.145	0.157	0.347	0.718	1.567	1.715
0.40	0.025	0.025	0.101	0.047	0.036	0.741	1.547	2.107

bias in 80 percent point (CENTIMETERS)

alpha*d= albedo	2.000	4.000	6.000	8.000	10.000	12.000	14.000	16.000
0.93	0.071	0.119	0.300	0.484	0.920	1.132	1.579	2.048
0.90	0.069	0.116	0.247	0.431	0.937	1.207	1.619	1.888
0.80	0.025	0.102	0.201	0.424	0.782	1.055	1.598	1.471
0.60	0.021	0.073	0.090	0.266	0.729	0.905	1.717	1.178
0.50	0.018	0.059	0.084	0.095	0.642	0.886	1.602	1.792
0.40	0.016	0.022	0.064	-0.032	0.402	1.018	1.525	2.311

rise time from one percent point to peak (ns)

alpha*d= albedo	2.000	4.000	6.000	8.000	10.000	12.000	14.000	16.000
0.93	-0.001	0.001	-0.002	0.440	-0.014	0.425	0.396	0.420
0.90	-0.000	0.001	-0.002	-0.004	-0.013	0.425	-0.046	0.420
0.80	-0.000	0.001	0.443	-0.003	-0.007	-0.016	0.382	0.416
0.60	-0.000	0.001	-0.001	-0.001	0.444	-0.011	0.415	-0.013
0.50	-0.000	0.000	-0.000	0.445	0.002	0.437	0.429	-0.006
0.40	-0.000	0.000	0.000	0.001	0.004	0.439	0.441	0.445

convolution summary for NOS water

zenith angle of entry= 0.00 degrees DEPTH= 20.00 METERS

INHOMOGENEITY MODEL NO. 4 RESULTS ARE RELATIVE TO THE HOMOGENEOUS CASE

bias in 10 percent point (CENTIMETERS)

alpha*d=	2.000	4.000	6.000	8.000	10.000	12.000	14.000	16.000
albedo								
0.93	-0.069	-0.195	-0.271	-0.451	-0.976	-0.988	-0.795	-1.391
0.90	-0.067	-0.187	-0.253	-0.468	-0.943	-0.906	-0.732	-1.296
0.80	-0.053	-0.162	-0.199	-0.396	-0.798	-0.764	-0.601	-0.881
0.60	-0.040	-0.116	-0.142	-0.252	-0.612	-0.537	-0.290	-0.205
0.50	-0.033	-0.094	-0.114	-0.224	-0.535	-0.406	-0.179	-0.124
0.40	-0.026	-0.063	-0.084	-0.185	-0.494	-0.297	-0.107	-0.090

bias in 20 percent point (CENTIMETERS)

alpha*d=	2.000	4.000	6.000	8.000	10.000	12.000	14.000	16.000
albedo								
0.93	-0.120	-0.288	-0.518	-0.624	-0.967	-1.165	-1.175	-1.866
0.90	-0.118	-0.280	-0.490	-0.614	-0.978	-1.155	-1.120	-1.727
0.80	-0.095	-0.254	-0.401	-0.569	-0.940	-0.953	-0.878	-1.376
0.60	-0.079	-0.202	-0.282	-0.378	-0.743	-0.655	-0.254	-0.365
0.50	-0.068	-0.175	-0.222	-0.308	-0.655	-0.474	-0.131	-0.119
0.40	-0.056	-0.128	-0.157	-0.259	-0.597	-0.300	-0.086	-0.033

bias in 50 percent point (CENTIMETERS)

alpha*d=	2.000	4.000	6.000	8.000	10.000	12.000	14.000	16.000
albedo								
0.93	-0.176	-0.392	-0.550	-0.702	-1.132	-1.317	-1.250	-2.096
0.90	-0.172	-0.385	-0.525	-0.706	-1.147	-1.241	-1.302	-2.021
0.80	-0.127	-0.360	-0.445	-0.640	-1.099	-1.138	-1.142	-1.582
0.60	-0.102	-0.302	-0.335	-0.470	-0.736	-0.927	-0.715	-0.454
0.50	-0.088	-0.270	-0.293	-0.370	-0.603	-0.786	-0.625	-0.250
0.40	-0.073	-0.187	-0.232	-0.342	-0.555	-0.530	-0.583	-0.210

bias in 80 percent point (CENTIMETERS)

alpha*d=	2.000	4.000	6.000	8.000	10.000	12.000	14.000	16.000
albedo								
0.93	-0.129	-0.234	-0.457	-0.685	-1.346	-1.878	-1.908	-3.017
0.90	-0.126	-0.234	-0.426	-0.696	-1.410	-1.785	-2.031	-2.996
0.80	-0.069	-0.233	-0.323	-0.582	-1.070	-1.417	-1.649	-2.115
0.60	-0.057	-0.217	-0.225	-0.322	-0.650	-0.894	-0.604	-0.238
0.50	-0.050	-0.201	-0.214	-0.188	-0.562	-0.703	-0.430	0.019
0.40	-0.042	-0.116	-0.192	-0.170	-0.578	-0.386	-0.337	0.047

rise time from one percent point to peak (ns)

alpha*d=	2.000	4.000	6.000	8.000	10.000	12.000	14.000	16.000
albedo								
0.93	0.000	0.002	-0.440	0.007	-0.423	-0.411	0.018	-0.403
0.90	0.000	0.002	0.004	0.006	0.021	0.030	-0.427	0.037
0.80	0.000	0.002	0.003	0.005	-0.427	-0.424	0.023	-0.397
0.60	0.000	0.001	0.002	0.003	0.013	0.009	0.013	-0.425
0.50	0.000	0.001	0.002	0.001	-0.433	0.005	0.012	0.458
0.40	0.000	0.000	0.002	0.000	0.011	0.002	0.010	0.009

convolution summary for NOS water

zenith angle of entry= 0.00 degrees DEPTH= 20.00 METERS

INHOMOGENEITY MODEL NO. 5 RESULTS ARE RELATIVE TO THE HOMOGENEOUS CASE

bias in 10 percent point (CENTIMETERS)

alpha*d= albedo	2.000	4.000	6.000	8.000	10.000	12.000	14.000	16.000
0.93	-0.221	-0.506	-0.812	-1.280	-2.140	-2.979	-2.804	-3.550
0.90	-0.213	-0.487	-0.768	-1.281	-2.050	-2.836	-2.771	-3.323
0.80	-0.173	-0.425	-0.609	-1.097	-1.771	-2.741	-2.208	-2.755
0.60	-0.134	-0.304	-0.429	-0.791	-1.439	-2.139	-1.265	-1.550
0.50	-0.114	-0.245	-0.338	-0.695	-1.275	-2.037	-0.872	-1.156
0.40	-0.093	-0.166	-0.244	-0.572	-1.259	-1.885	-0.671	-0.896

bias in 20 percent point (CENTIMETERS)

alpha*d= albedo	2.000	4.000	6.000	8.000	10.000	12.000	14.000	16.000
0.93	-0.357	-0.757	-1.302	-1.563	-2.263	-3.463	-3.454	-4.290
0.90	-0.344	-0.736	-1.244	-1.533	-2.256	-3.403	-3.354	-4.190
0.80	-0.279	-0.663	-1.023	-1.415	-2.044	-3.131	-3.051	-3.514
0.60	-0.226	-0.508	-0.743	-1.062	-1.636	-2.590	-1.634	-2.063
0.50	-0.193	-0.424	-0.609	-0.843	-1.416	-2.369	-1.134	-1.600
0.40	-0.158	-0.298	-0.458	-0.697	-1.372	-2.164	-0.916	-1.398

bias in 50 percent point (CENTIMETERS)

alpha*d= albedo	2.000	4.000	6.000	8.000	10.000	12.000	14.000	16.000
0.93	-0.509	-0.865	-1.499	-2.041	-2.804	-3.758	-3.598	-4.873
0.90	-0.487	-0.855	-1.436	-1.986	-2.773	-3.659	-3.638	-4.757
0.80	-0.363	-0.815	-1.184	-1.720	-2.530	-3.402	-3.484	-4.034
0.60	-0.289	-0.697	-0.843	-1.248	-1.887	-2.867	-2.559	-2.432
0.50	-0.248	-0.617	-0.755	-0.870	-1.568	-2.581	-2.220	-1.914
0.40	-0.206	-0.418	-0.635	-0.748	-1.443	-2.233	-1.897	-1.573

bias in 80 percent point (CENTIMETERS)

alpha*d= albedo	2.000	4.000	6.000	8.000	10.000	12.000	14.000	16.000
0.93	-0.367	-0.528	-1.368	-2.023	-3.323	-4.890	-5.139	-6.954
0.90	-0.345	-0.529	-1.299	-1.936	-3.086	-4.589	-5.068	-6.849
0.80	-0.197	-0.526	-0.964	-1.604	-2.525	-3.962	-4.275	-5.573
0.60	-0.163	-0.482	-0.593	-1.085	-1.740	-2.830	-2.192	-2.299
0.50	-0.143	-0.437	-0.547	-0.658	-1.385	-2.450	-1.720	-1.526
0.40	-0.121	-0.228	-0.476	-0.623	-1.331	-2.083	-1.268	-1.142

rise time from one percent point to peak (ns)

alpha*d= albedo	2.000	4.000	6.000	8.000	10.000	12.000	14.000	16.000
0.93	0.002	0.007	-0.433	0.024	-0.833	-0.336	-0.370	-0.778
0.90	-0.442	0.006	-0.434	-0.422	-0.392	-0.345	-0.797	-0.345
0.80	0.002	0.005	0.008	-0.426	-0.405	-0.370	-0.374	-0.320
0.60	0.001	0.003	0.005	0.011	0.024	-0.404	0.023	-0.385
0.50	0.001	0.002	0.004	0.008	-0.426	-0.417	0.011	-0.399
0.40	0.001	0.001	0.003	0.006	-0.429	0.015	-0.441	0.036

convolution summary for NOS water

zenith angle of entry= 25.00 degrees DEPTH= 20.00 METERS

INHOMOGENEITY MODEL NO. 1 RESULTS ARE FOR ABSOLUTE BIASES AND RISE TIMES

bias in 10 percent point (CENTIMETERS)

alpha*d= / albedo	2.000	4.000	6.000	8.000	10.000	12.000	14.000	16.000
0.93	-57.638	-59.406	-60.883	-61.850	-61.451	-59.776	-58.805	-55.808
0.90	-57.587	-59.317	-60.851	-61.954	-61.750	-60.285	-59.523	-56.768
0.80	-57.418	-58.982	-60.659	-62.079	-62.483	-61.592	-61.183	-59.399
0.60	-57.068	-58.182	-59.770	-61.217	-62.588	-61.837	-61.041	-60.202
0.50	-56.900	-57.760	-59.106	-60.415	-61.854	-60.485	-59.497	-58.642
0.40	-56.747	-57.359	-58.335	-59.340	-60.754	-58.744	-57.889	-57.257

bias in 20 percent point (CENTIMETERS)

alpha*d= / albedo	2.000	4.000	6.000	8.000	10.000	12.000	14.000	16.000
0.93	-56.687	-57.199	-57.481	-57.670	-56.552	-54.178	-53.187	-49.901
0.90	-56.681	-57.190	-57.555	-57.885	-56.957	-54.890	-54.107	-51.270
0.80	-56.661	-57.128	-57.736	-58.411	-58.071	-56.916	-56.643	-54.782
0.60	-56.584	-56.904	-57.648	-58.595	-59.128	-58.691	-58.667	-58.313
0.50	-56.537	-56.777	-57.427	-58.286	-59.096	-58.567	-58.487	-58.035
0.40	-56.499	-56.669	-57.124	-57.759	-58.766	-57.995	-57.741	-57.233

bias in 50 percent point (CENTIMETERS)

alpha*d= / albedo	2.000	4.000	6.000	8.000	10.000	12.000	14.000	16.000
0.93	-57.178	-57.095	-56.654	-55.998	-54.003	-50.514	-49.043	-45.337
0.90	-57.195	-57.139	-56.839	-56.376	-54.583	-51.463	-50.380	-47.158
0.80	-57.251	-57.251	-57.402	-57.439	-56.292	-54.218	-54.047	-52.131
0.60	-57.248	-57.344	-57.969	-58.590	-58.484	-57.557	-58.039	-57.720
0.50	-57.200	-57.355	-58.026	-58.687	-58.923	-58.241	-58.754	-58.164
0.40	-57.148	-57.372	-57.962	-58.518	-59.027	-58.377	-58.326	-57.632

bias in 80 percent point (CENTIMETERS)

alpha*d= / albedo	2.000	4.000	6.000	8.000	10.000	12.000	14.000	16.000
0.93	-58.680	-58.600	-58.122	-57.175	-54.325	-49.464	-47.600	-42.958
0.90	-58.687	-58.638	-58.327	-57.630	-55.085	-50.783	-49.424	-45.676
0.80	-58.710	-58.727	-58.970	-58.931	-57.361	-54.541	-54.500	-52.722
0.60	-58.560	-58.762	-59.513	-60.258	-60.089	-58.966	-59.769	-59.430
0.50	-58.403	-58.736	-59.504	-60.303	-60.509	-59.747	-60.445	-59.300
0.40	-58.232	-58.708	-59.361	-60.058	-60.505	-59.734	-59.361	-58.232

rise time from one percent point to peak (ns)

alpha*d= / albedo	2.000	4.000	6.000	8.000	10.000	12.000	14.000	16.000
0.93	8.806	9.304	9.881	10.387	10.834	11.654	12.005	12.690
0.90	8.782	9.290	9.878	10.396	10.852	11.687	12.035	12.291
0.80	8.690	9.228	9.859	9.971	10.455	10.872	10.784	11.050
0.60	7.994	9.020	9.328	9.493	10.044	9.937	9.311	9.146
0.50	7.841	8.875	9.238	9.410	9.571	9.302	8.967	8.329
0.40	7.614	8.684	9.069	9.268	9.480	8.389	8.032	7.459

convolution summary for NOS water

zenith angle of entry= 25.00 degrees DEPTH= 20.00 METERS

INHOMOGENEITY MODEL NO. 2 RESULTS ARE RELATIVE TO THE HOMOGENEOUS CASE

bias in 10 percent point (CENTIMETERS)

alpha*d= / albedo	2.000	4.000	6.000	8.000	10.000	12.000	14.000	16.000
0.93	-0.481	-0.937	-1.591	-1.770	-1.809	-1.656	-1.779	-1.563
0.90	-0.465	-0.912	-1.552	-1.744	-1.780	-1.711	-1.705	-1.631
0.80	-0.409	-0.824	-1.377	-1.639	-1.683	-1.758	-1.675	-1.418
0.60	-0.296	-0.624	-0.946	-1.366	-1.471	-1.319	-1.027	-0.803
0.50	-0.242	-0.515	-0.788	-0.910	-1.319	-0.702	-0.464	-0.368
0.40	-0.190	-0.404	-0.616	-0.732	-0.858	-0.293	-0.193	-0.105

bias in 20 percent point (CENTIMETERS)

alpha*d= / albedo	2.000	4.000	6.000	8.000	10.000	12.000	14.000	16.000
0.93	-0.426	-0.807	-1.197	-1.371	-1.488	-1.499	-1.641	-1.539
0.90	-0.412	-0.784	-1.164	-1.340	-1.463	-1.501	-1.658	-1.428
0.80	-0.367	-0.706	-1.046	-1.246	-1.378	-1.319	-1.382	-1.357
0.60	-0.267	-0.536	-0.770	-0.952	-1.225	-0.821	-0.851	-0.849
0.50	-0.222	-0.446	-0.624	-0.776	-1.041	-0.493	-0.464	-0.430
0.40	-0.177	-0.355	-0.473	-0.618	-0.789	-0.159	-0.191	-0.134

bias in 50 percent point (CENTIMETERS)

alpha*d= / albedo	2.000	4.000	6.000	8.000	10.000	12.000	14.000	16.000
0.93	-0.447	-0.767	-1.073	-1.170	-1.216	-1.261	-1.686	-1.407
0.90	-0.434	-0.749	-1.049	-1.153	-1.206	-1.262	-1.654	-1.341
0.80	-0.390	-0.686	-0.960	-1.064	-1.155	-1.239	-1.403	-1.275
0.60	-0.284	-0.541	-0.710	-0.829	-1.025	-0.984	-0.944	-1.027
0.50	-0.239	-0.460	-0.573	-0.688	-0.913	-0.784	-0.506	-0.585
0.40	-0.194	-0.376	-0.429	-0.546	-0.775	-0.402	-0.199	-0.198

bias in 80 percent point (CENTIMETERS)

alpha*d= / albedo	2.000	4.000	6.000	8.000	10.000	12.000	14.000	16.000
0.93	-0.318	-0.559	-0.791	-0.826	-0.832	-0.687	-1.215	-1.184
0.90	-0.309	-0.549	-0.784	-0.843	-0.862	-0.723	-1.295	-1.040
0.80	-0.279	-0.513	-0.744	-0.816	-0.825	-0.694	-1.072	-0.793
0.60	-0.190	-0.423	-0.568	-0.686	-0.727	-0.474	-0.800	-0.609
0.50	-0.161	-0.370	-0.475	-0.581	-0.595	-0.431	-0.376	-0.314
0.40	-0.130	-0.312	-0.373	-0.469	-0.432	-0.190	-0.130	-0.099

rise time from one percent point to peak (ns)

alpha*d= / albedo	2.000	4.000	6.000	8.000	10.000	12.000	14.000	16.000
0.93	0.163	0.201	0.228	0.206	0.204	0.208	0.161	-0.258
0.90	0.160	0.197	0.229	0.204	0.201	0.200	-0.279	-0.268
0.80	0.167	0.181	0.232	0.200	0.193	0.181	0.147	0.178
0.60	0.157	0.204	0.217	0.204	0.198	0.170	0.075	0.161
0.50	0.139	0.193	0.196	0.216	0.216	0.147	-0.380	0.114
0.40	0.155	0.181	0.210	0.185	0.248	0.122	0.023	0.083

convolution summary for NOS water

zenith angle of entry= 25.00 degrees DEPTH= 20.00 METERS

INHOMOGENEITY MODEL NO. 3 RESULTS ARE RELATIVE TO THE HOMOGENEOUS CASE

bias in 10 percent point (CENTIMETERS)

alpha*d= albedo	2.000	4.000	6.000	8.000	10.000	12.000	14.000	16.000
0.93	-1.239	-2.580	-3.855	-4.113	-4.390	-4.309	-4.208	-4.260
0.90	-1.198	-2.466	-3.782	-4.068	-4.338	-4.315	-4.190	-4.108
0.80	-1.058	-2.131	-3.485	-3.880	-4.259	-4.203	-4.057	-3.569
0.60	-0.766	-1.650	-2.487	-3.421	-3.686	-3.550	-3.620	-1.973
0.50	-0.630	-1.383	-1.861	-2.823	-3.269	-2.679	-2.120	-0.797
0.40	-0.496	-1.103	-1.439	-1.901	-2.518	-1.313	-1.062	-0.250

bias in 20 percent point (CENTIMETERS)

alpha*d= albedo	2.000	4.000	6.000	8.000	10.000	12.000	14.000	16.000
0.93	-1.102	-2.084	-3.022	-3.514	-3.832	-3.915	-3.994	-4.032
0.90	-1.066	-2.028	-2.943	-3.468	-3.822	-3.853	-3.911	-3.757
0.80	-0.948	-1.834	-2.650	-3.220	-3.717	-3.589	-3.509	-3.218
0.60	-0.690	-1.420	-1.911	-2.555	-3.191	-2.850	-2.967	-1.752
0.50	-0.574	-1.200	-1.537	-2.119	-2.715	-2.137	-2.104	-0.836
0.40	-0.459	-0.972	-1.169	-1.598	-2.104	-1.208	-1.105	-0.286

bias in 50 percent point (CENTIMETERS)

alpha*d= albedo	2.000	4.000	6.000	8.000	10.000	12.000	14.000	16.000
0.93	-1.164	-2.035	-2.644	-2.987	-3.372	-3.479	-4.184	-4.406
0.90	-1.130	-1.989	-2.585	-2.955	-3.347	-3.475	-4.068	-4.106
0.80	-1.013	-1.827	-2.358	-2.722	-3.264	-3.322	-3.524	-3.270
0.60	-0.728	-1.457	-1.759	-2.143	-2.911	-2.942	-3.091	-2.115
0.50	-0.613	-1.253	-1.433	-1.812	-2.584	-2.461	-2.315	-1.169
0.40	-0.497	-1.036	-1.086	-1.439	-2.179	-1.588	-1.304	-0.427

bias in 80 percent point (CENTIMETERS)

alpha*d= albedo	2.000	4.000	6.000	8.000	10.000	12.000	14.000	16.000
0.93	-0.806	-1.509	-1.954	-2.108	-2.421	-2.539	-3.686	-4.136
0.90	-0.782	-1.480	-1.938	-2.140	-2.429	-2.487	-3.582	-3.532
0.80	-0.703	-1.376	-1.841	-2.033	-2.444	-2.380	-2.913	-2.283
0.60	-0.457	-1.130	-1.407	-1.655	-2.354	-2.219	-2.706	-1.323
0.50	-0.383	-0.988	-1.164	-1.441	-2.073	-1.987	-1.939	-0.542
0.40	-0.308	-0.833	-0.901	-1.189	-1.747	-1.303	-0.980	-0.137

rise time from one percent point to peak (ns)

alpha*d= albedo	2.000	4.000	6.000	8.000	10.000	12.000	14.000	16.000
0.93	0.449	0.479	0.476	0.485	0.462	0.412	0.377	-0.450
0.90	0.446	0.479	0.475	0.484	0.457	-0.035	-0.071	-0.017
0.80	0.436	0.479	0.470	0.477	0.441	0.402	0.341	-0.040
0.60	0.409	0.482	0.453	0.466	-0.045	0.368	0.353	0.405
0.50	0.378	0.470	0.446	0.465	0.379	0.362	-0.058	0.417
0.40	0.367	0.465	0.436	0.460	0.366	0.348	0.402	0.334

convolution summary for NOS water

zenith angle of entry= 25.00 degrees DEPTH= 20.00 METERS

INHOMOGENEITY MODEL NO. 4 RESULTS ARE RELATIVE TO THE HOMOGENEOUS CASE

bias in 10 percent point (CENTIMETERS)

alpha*d= / albedo	2.000	4.000	6.000	8.000	10.000	12.000	14.000	16.000
0.93	0.383	0.607	0.780	0.719	0.685	0.295	0.161	-0.087
0.90	0.371	0.593	0.769	0.738	0.744	0.317	0.191	-0.069
0.80	0.331	0.540	0.722	0.777	0.866	0.482	0.315	0.021
0.60	0.245	0.411	0.585	0.552	1.014	0.706	0.537	0.011
0.50	0.204	0.337	0.484	0.488	0.967	0.604	0.561	-0.004
0.40	0.162	0.259	0.363	0.393	0.827	0.491	0.387	0.006

bias in 20 percent point (CENTIMETERS)

alpha*d= / albedo	2.000	4.000	6.000	8.000	10.000	12.000	14.000	16.000
0.93	0.319	0.470	0.595	0.527	0.476	0.090	0.251	-0.423
0.90	0.310	0.457	0.582	0.532	0.480	0.131	0.262	-0.345
0.80	0.279	0.411	0.533	0.562	0.524	0.294	0.380	-0.123
0.60	0.210	0.306	0.406	0.495	0.627	0.511	0.633	0.028
0.50	0.178	0.250	0.320	0.427	0.699	0.592	0.649	-0.003
0.40	0.146	0.193	0.223	0.331	0.740	0.520	0.444	0.002

bias in 50 percent point (CENTIMETERS)

alpha*d= / albedo	2.000	4.000	6.000	8.000	10.000	12.000	14.000	16.000
0.93	0.298	0.432	0.432	0.325	0.108	-0.348	0.270	-0.391
0.90	0.292	0.426	0.426	0.334	0.099	-0.289	0.317	-0.347
0.80	0.269	0.398	0.400	0.395	0.129	0.011	0.501	-0.135
0.60	0.204	0.316	0.337	0.339	0.239	0.466	0.624	0.098
0.50	0.177	0.265	0.280	0.283	0.340	0.688	0.649	0.046
0.40	0.148	0.210	0.215	0.210	0.403	0.671	0.462	0.031

bias in 80 percent point (CENTIMETERS)

alpha*d= / albedo	2.000	4.000	6.000	8.000	10.000	12.000	14.000	16.000
0.93	0.285	0.352	0.404	0.197	-0.127	-0.939	0.075	-0.852
0.90	0.279	0.350	0.401	0.218	-0.138	-0.889	0.096	-0.716
0.80	0.258	0.334	0.391	0.358	-0.037	-0.383	0.249	-0.128
0.60	0.187	0.273	0.391	0.349	0.256	0.235	0.449	0.256
0.50	0.163	0.231	0.354	0.311	0.461	0.508	0.536	0.056
0.40	0.136	0.183	0.297	0.243	0.569	0.533	0.325	-0.001

rise time from one percent point to peak (ns)

alpha*d= / albedo	2.000	4.000	6.000	8.000	10.000	12.000	14.000	16.000
0.93	-0.090	-0.090	-0.067	-0.059	-0.050	-0.031	-0.015	-0.002
0.90	-0.093	-0.090	-0.067	-0.058	-0.049	-0.475	-0.013	0.002
0.80	-0.103	-0.094	-0.063	-0.058	-0.046	-0.026	-0.015	0.015
0.60	-0.090	-0.097	-0.068	-0.063	-0.484	-0.013	-0.023	0.051
0.50	-0.106	-0.087	-0.077	-0.053	-0.037	-0.009	-0.107	0.025
0.40	-0.082	-0.105	-0.094	-0.061	-0.036	-0.028	-0.217	0.028

convolution summary for NOS water

zenith angle of entry= 25.00 degrees DEPTH= 20.00 METERS

INHOMOGENEITY MODEL NO. 5 RESULTS ARE RELATIVE TO THE HOMOGENEOUS CASE

bias in 10 percent point (CENTIMETERS)

alpha*d=	2.000	4.000	6.000	8.000	10.000	12.000	14.000	16.000
albedo								
0.93	0.946	1.560	1.966	1.959	1.458	0.912	0.691	0.018
0.90	0.915	1.526	1.936	1.969	1.520	0.977	0.782	0.186
0.80	0.808	1.400	1.814	1.990	1.761	1.246	1.042	0.554
0.60	0.574	1.091	1.487	1.636	1.957	1.532	1.253	0.653
0.50	0.465	0.911	1.255	1.449	1.792	1.346	1.122	0.399
0.40	0.362	0.720	0.986	1.175	1.529	1.018	0.714	0.179

bias in 20 percent point (CENTIMETERS)

alpha*d=	2.000	4.000	6.000	8.000	10.000	12.000	14.000	16.000
albedo								
0.93	0.766	1.204	1.464	1.559	1.012	0.418	0.591	-0.056
0.90	0.741	1.176	1.430	1.547	1.018	0.550	0.703	0.135
0.80	0.659	1.073	1.306	1.540	1.144	0.898	1.096	0.542
0.60	0.483	0.828	1.029	1.297	1.302	1.195	1.375	0.815
0.50	0.402	0.693	0.844	1.098	1.296	1.244	1.296	0.491
0.40	0.322	0.552	0.641	0.840	1.189	1.026	0.863	0.208

bias in 50 percent point (CENTIMETERS)

alpha*d=	2.000	4.000	6.000	8.000	10.000	12.000	14.000	16.000
albedo								
0.93	0.680	1.037	1.096	0.993	0.261	-0.786	-0.426	-0.546
0.90	0.661	1.022	1.075	0.983	0.244	-0.669	-0.191	-0.208
0.80	0.595	0.958	1.002	1.029	0.373	-0.212	0.502	0.519
0.60	0.429	0.773	0.893	0.857	0.594	0.553	1.179	1.040
0.50	0.362	0.656	0.781	0.720	0.653	0.954	1.335	0.622
0.40	0.293	0.528	0.646	0.545	0.635	1.007	0.981	0.268

bias in 80 percent point (CENTIMETERS)

alpha*d=	2.000	4.000	6.000	8.000	10.000	12.000	14.000	16.000
albedo								
0.93	0.668	0.910	1.031	0.872	-0.388	-2.118	-1.226	-1.944
0.90	0.652	0.902	1.017	0.840	-0.381	-1.865	-0.924	-1.347
0.80	0.596	0.864	0.972	1.006	-0.025	-0.985	0.066	0.075
0.60	0.426	0.729	0.971	0.934	0.515	0.167	0.843	0.791
0.50	0.364	0.637	0.886	0.836	0.683	0.719	1.060	0.336
0.40	0.299	0.533	0.766	0.682	0.716	0.858	0.767	0.098

rise time from one percent point to peak (ns)

alpha*d=	2.000	4.000	6.000	8.000	10.000	12.000	14.000	16.000
albedo								
0.93	-0.263	-0.222	-0.170	-0.152	-0.136	-0.544	-0.485	-0.908
0.90	-0.269	-0.226	-0.171	-0.155	-0.585	-0.998	-0.929	-0.457
0.80	-0.257	-0.241	-0.172	-0.163	-0.144	-0.117	-0.058	0.015
0.60	-0.247	-0.226	-0.192	-0.165	-0.575	-0.534	-0.025	0.037
0.50	-0.265	-0.239	-0.214	-0.159	-0.121	-0.054	-0.097	-0.085
0.40	-0.224	-0.253	-0.210	-0.195	-0.105	-0.057	-0.434	-0.110

NOAA SCIENTIFIC AND TECHNICAL PUBLICATIONS

The National Oceanic and Atmospheric Administration was established as part of the Department of Commerce on October 3, 1970. The mission responsibilities of NOAA are to assess the socioeconomic impact of natural and technological changes in the environment and to monitor and predict the state of the solid Earth, the oceans and their living resources, the atmosphere, and the space environment of the Earth.

The major components of NOAA regularly produce various types of scientific and technical information in the following kinds of publications:

PROFESSIONAL PAPERS — Important definitive research results, major techniques, and special investigations.

CONTRACT AND GRANT REPORTS — Reports prepared by contractors or grantees under NOAA sponsorship.

ATLAS — Presentation of analyzed data generally in the form of maps showing distribution of rainfall, chemical and physical conditions of oceans and atmosphere, distribution of fishes and marine mammals, ionospheric conditions, etc.

TECHNICAL SERVICE PUBLICATIONS — Reports containing data, observations, instructions, etc. A partial listing includes data serials; prediction and outlook periodicals; technical manuals, training papers, planning reports, and information serials; and miscellaneous technical publications.

TECHNICAL REPORTS — Journal quality with extensive details, mathematical developments, or data listings.

TECHNICAL MEMORANDUMS — Reports of preliminary, partial, or negative research or technology results, interim instructions, and the like.

Information on availability of NOAA publications can be obtained from:

ENVIRONMENTAL SCIENCE INFORMATION CENTER (D822)
ENVIRONMENTAL DATA AND INFORMATION SERVICE
NATIONAL OCEANIC AND ATMOSPHERIC ADMINISTRATION
U.S. DEPARTMENT OF COMMERCE

6009 Executive Boulevard
Rockville, MD 20852

NOAA--S/T 81-249